Ultrasound flow investigations at a zinc-air flow battery model

Christian Kupsch[1*]**, Lukas Feierabend**[2]**, Richard Nauber**[1]**, Lars Büttner**[1]**,
Jürgen Czarske**[1]

[1] Technische Universität Dresden, Laboratory for Measurement and Sensor System Techniques, 01062 Dresden, Germany

[2] ZBT GmbH, Carl-Benz-Strasse 201, 47057 Duisburg, Germany

* christian.kupsch@tu-dresden.de

Abstract

The investigation of suspension flows with moderately high particle concentration (in the order of 10 vol.-%) is relevant for a wide range of industrial processes. For example, the performance of zinc-air flow batteries (ZABs) depends on the local flow conditions of the suspension electrode (a suspension of microscopic zinc particles in an aqueous potassium hydroxide solution with a gelling agent) in the electrochemical cell. It is crucial to understand and model the flow of such opaque and multiphase fluids, which requires flow measurements.

We present an experiment for the validation of numerical models, including a measurement system based on ultrasound for flow mapping in multiphase fluids with a moderately high volume concentration of the suspended phase. The investigated flow channel is a scaled fluidic model of a ZAB. The utilized measurement system based on ultrasound imaging velocimetry is validated with optical reference measurements and CFD simulations for the model fluid glycerin. Finally the measured flow field of the suspension electrode in the fluidic model is compared to results from a numeric simulation, which demonstrates the necessity and applicability of the measurement technique.

1 Introduction

Zinc-air flow batteries are a promising candidate for large-scale stationary and mobile energy storage systems due to the decoupling of of energy capacity and power density, a high gravimetric energy density and the low costs of the active base material zinc (Sapkota and Kim, 2009). They are operated by pumping a suspension of zinc particles and an aqueous potassium hydroxide solution with a gelling agent, called zinc-slurry, through an electrochemical cell. To fully exploit their theoretical potential, the flow field has to be optimized (Smith et al., 2014). For a structured layout process of zinc-air flow batteries, numerical simulations of the suspension flow are essential. Due to the complexity of the non-Newtonian multiphase fluid with high particle loadings, numerical simulations are non-trivial. The electrolyte with the gelling agent is by itself a complex fluid, sometimes called microgel (Piau, 2007), with non-Newtonian flow characteristics. Considering the additional particle content including particle-particle-interactions increases the overall complexity to accurately represent the flow behaviour with numerical methods. Aside from a typical macrohomogeneous approach with adapted constitutional laws (rheology model and wall functions), a more detailed method that directly considers local particle-particle-and particle-fluid interactions through coupling of computational fluid dynamics with the discrete element method (DEM) (Deen et al., 2007) could be investigated. All of the considered computational methods still require experimental validation. In the literature, local flow measurement data of opaque, viscous, non-Newtonian liquids with particles is sparse. Ultrasound Doppler velocimetry is commonly used to measure flow fields in opaque liquids (Thieme et al., 2017; Nauber et al., 2018; Büttner et al., 2013). Due to the high particle concentration in the zinc slurry, scattering and wave front distortions are introduced, which impact especially the phase of the received signals. This results in a significant increase of the measurement uncertainty for Doppler based velocity estimation. In recent years, an alternative ultrasound flow imaging technique was investigated: the ultrasound imaging velocimetry (UIV). UIV uses a correlation based velocity estimation comparable to optical PIV, but operates

on echographic images (Poelma, 2017). Since it is an intensity based velcoity estimation it is assumed to be more robust against the wave front distortions. To our knowledge, the UIV was not applied to a fluid with high contrast in density between the phases and a high particle concentration like the zinc-slurry until now. We present an experiment for the validation of numerical models, including a measurement system based on ultrasound for flow imaging in multiphase fluids with a moderately high volume concentration of the suspended phase. The flow of zinc slurry in a fluidic model of a ZAB is measured using ultrasound image velocimetry. For validation of the measurement system, glycerin flow is measured with the UIV and optical PIV in parallel. The measurement results demonstrate the usability of the measurement system for flow mapping in opaque multiphase fluids and will be used to calibrate and validate numerical models.

2 Experimental setup and measurement priciple

2.1 Fluidic model of a ZAB

The setup for the flow measurement in the fluidic model of a ZAB is shown in Figure 1. Active ZABs usually have a small gap width between the current collector and the cathode or separator, respectively, to reduce the electrolyte resistance. Considering particle sizes and pressure drops for the fluidic system, this typically leads to gap widths between 2 mm and 5 mm. In order to validate the simulation with sufficient measurement points, a scaled flow channel was chosen for the fluidic model with a gap width of 15 mm. The walls are 4 mm thick and consist of PMMA. The measurement region is indicated by the red rectangle with a size of $15 \times 20 \, \text{mm}^2$. A high depth-to-width ratio of approximately 3 (resulting in a channel depth of 47 mm) was chosen to ensure little variation of the flow field along the elevation direction within the measurement region.

From the asymmetric inlet conditions, the flow changes into a fully developed flow further down the channel. For validating the numerical simulations, the fully developed flow profiles are compared. Furthermore the transition of the flow from the asymmetric inlet conditions to the symmetric flow profile can be analyzed.

2.2 Zinc suspension

The zinc suspension is an opaque slurry of non-spherical zinc (Zn) particles in an aqueous potassium hydroxide (KOH) solution with a polymeric gelling agent, i.e. polyacrylic acid (PAA). Furthermore, zinc oxide (ZnO) is added to the slurry to prevent self-discharge and the formation of hydrogen. The detailed composition of the fluid is listed in Table 2. The size distribution of the zinc particles (Grillo-Werke AG) is depicted in Table 1. The described zinc-slurry is applicable in active ZABs.
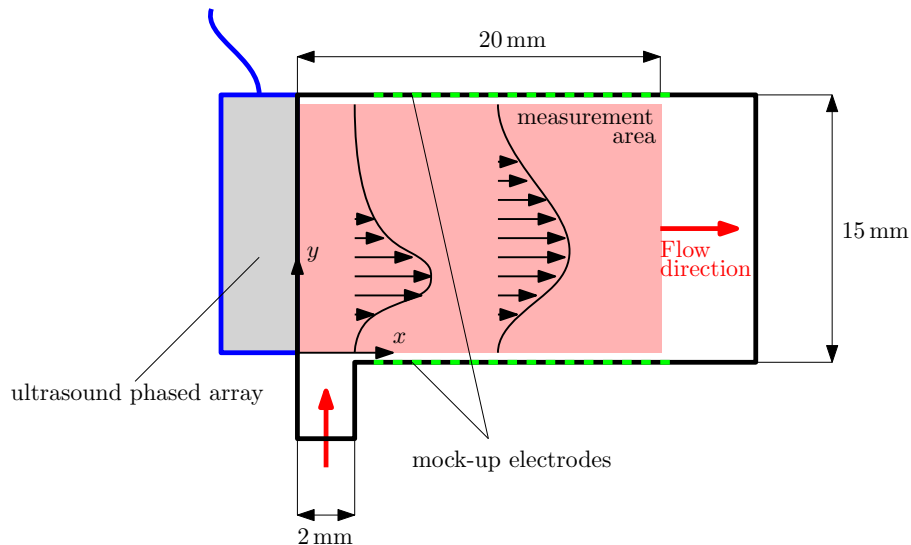

Figure 1: Scheme of the scaled fluidic model of a ZAB.

Table 1: Size distribution of the zinc particles.

Size range	$[25, 45]\,\mu m$	$[45, 63]\,\mu m$	$> 63\,\mu m$
Mass fraction in wt.-%	20	68	12

Table 2: Composition of the zinc-slurry.

Substance	Zn	KOH	ZnO	PAA	H_2O
Mass fraction in wt.-%	33.8	19.9	4	0.7	41.7

2.3 Ultrasound imaging velocimetry

The UIV technique images the speckle pattern induced by the particles in the multiphase fluid first. Using ultrafast imaging (Tanter and Fink, 2014), the medium is insonified with a plane wave and the scattered acoustic waves are recorded with a linear ultrasound array simultaneously for the whole measurement region. Subsequently a receive-side beamforming of the recorded signals is performed using the Delay-and-sum beamformer. If the volume fraction of particles is sufficiently high, the scattered waves from closely located particles superimpose and characteristic speckle patterns are visible in the acquired image. With a single transmission, a whole field is captured, which allows for high frame rates. Compared to images of particles, speckle images decorrelate much faster due to relative movements of the particles (Bohs et al., 2000). As a consequence, a high frame rate is indispensable to find a correlation in subsequent images and estimate the flow velocity.

Velocity estimation is done by splitting the recorded images into so-called interrogation windows and cross-correlating subsequent images. From the estimated displacement of the particles or speckles in every interrogation window, the velocity v in x and y direction can be calculated using the known inter-frame time. For a more detailed description, see (Adrian, 2005; Poelma, 2017). A number of $n_{epp} - 1$ (number of burst emissions per profile) calculated correlation functions are averaged to estimate the particle displacement Δx and Δy and the velocity components v_x and v_y can be calculated for one velocity frame. A number of N_{avg} of these velocity frames are then averaged using the median.

3 Validation of UIV

To validate the ultrasound measurement, it is compared to optical PIV measurements and CFD simulations for a model fluid. Glycerin is chosen for a validation measurement due to its transparency, a similar speed of sound compared to the zinc-slurry and high viscosity, which results in a laminar stationary flow with negligible turbulence.

Ultrasound measurement: To measure the flow field in the fluidic model, an ultrasound phased array transducer is attached to the left side, see Figure 1. The x- and y-component of the flow are measured in the measurement region. To drive the ultrasound transducers, an in-house developed research platform, the phased array ultrasound Doppler velocimeter (PAUDV) (Mäder et al., 2017) is used. A number of 50 ultrasound elements with a pitch of 0.3 mm and a height of 3 mm is used to excite an 6 MHz ultrasound signal with 2 periods. With a pulse repetition frequency of 600 Hz, the measurement is repeated for 50 s. The received signals are beamformed and a correlation based velocity estimation (Taylor et al., 2010) is applied. The interrogation windows have a size of ≈ 1 mm, which defines the achieved spatial resolution. 500 correlation pairs are averaged for a single velocity estimate. Subsequently, $N_{avg} = 20$ velocity estimates are averaged to find the mean velocity field.

Optical measurement: Laser light (561 nm) is transformed into a light sheet by a cylindrical lens, which covers the whole measurement region. Light is scattered by seeding particles (10 µm silver coated hollow glass spheres, Dantec Dynamcs) and focused onto a CCD camera. A number of 15000 pictures with a frame rate of 100 Hz and an exposure time of 0.4 ms are recorded. Similarly to the ultrasound measurement, a correlation based velocity estimation (Taylor et al., 2010) is applied with an interrogation window size of 0.53 mm.

CFD simulation: A CFD simulation was conducted using the finite volume CFD package OpenFOAM

(Weller et al., 1998).

The measured flow field and selected profiles of the x-component at different x-positions are depicted in Figure 3. Qualitatively the flow fields coincide well. From the profiles it can be seen, that at the high velocity inlet the velocity is underestimated by the ultrasound measurement. This is due to the high gradient and the lower resolution of the ultrasound measurement, which results in a spatial averaging and thereby a lower estimated velocity. For $x > 5$ mm the deviation of the ultrasound measurement from the optical measurement is smaller than 15 %. Besides underestimation of the velocity at high velocity inlet, the ultrasound measurement using UIV is considered validated.
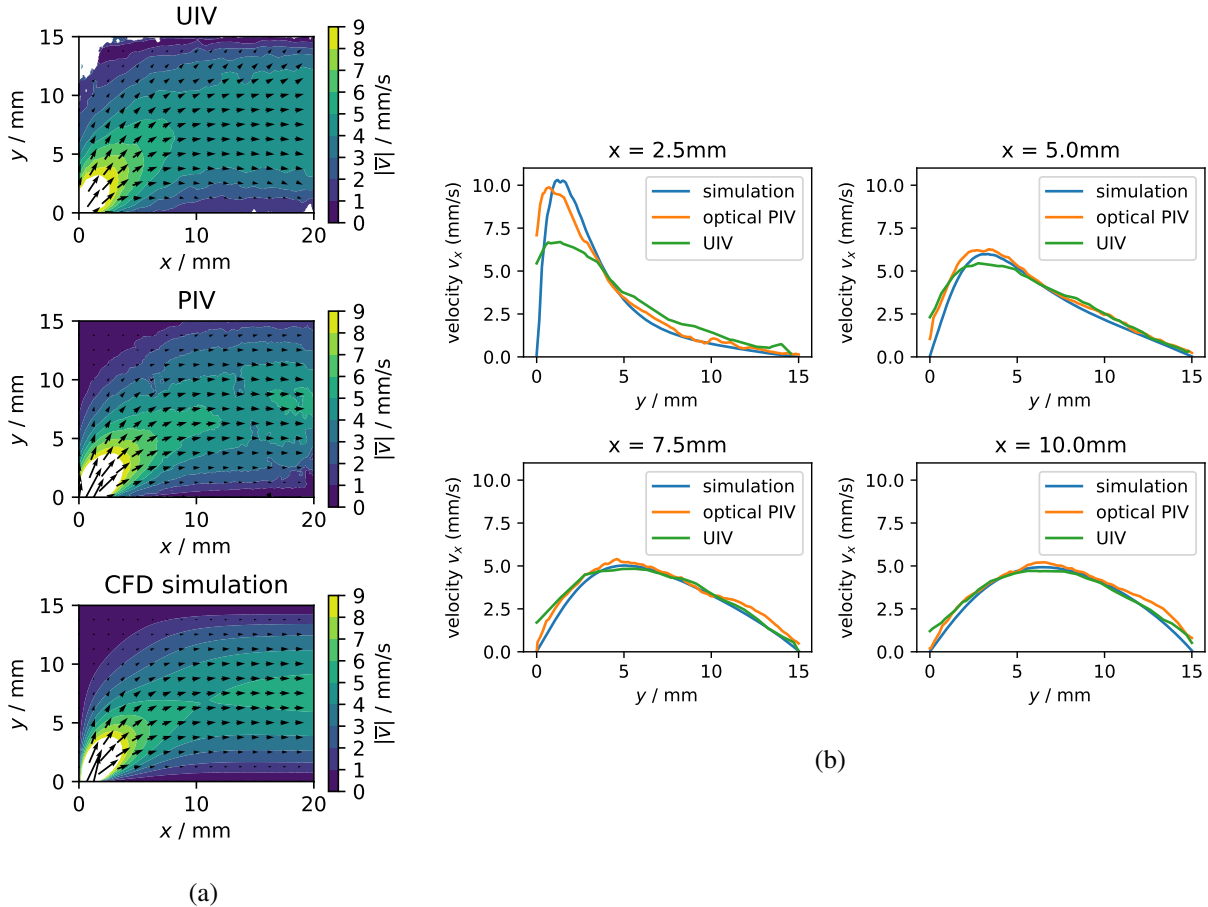

(a)

(b)

Figure 2: (a) Measured flow field for UIV, PIV and CFD simulated flow field of glycerin in the fluidic ZAB model. (b) Flow profiles of the x-component of the flow for selected x-positions for all three modalities.

4   Flow measurement

From the measurement data depicted in Figure 3a, it is evident that the slurry has significantly different flow characteristics compared to the Newtonian reference (glycerin). Opposite to the flow inlet at the top left corner (low x values, high y values), an extended zero-shear zone can be observed. This is assumed to result from Bingham-type rheological behavior with a pronounced yield stress, where the shear stress needs to exceed this critical yield stress in order to induce plastic shear in the fluid. After entering the flow channel, the pronounced yield stress and the wall slip cause the flow to immediately turn into the main flow direction and proceed along the entrance wall.

The wall slip is displayed in Figure 3b, where velocity profiles are extracted at representative positions of the the x-direction. The gelled electrolyte without particles show significant wall slip. This has been observed for microgels with polyacrylic acid binder before (Piau, 2007) and a suspension with particles should even enhance these properties.

A replication of the measured flow characteristics was attempted with numerical simulations of a single-phase, generalized Newtonian fluid with wall slip. The generalized Newtonian flow model assumes that the viscosity is only a function of the apparent shear rate, but not of its shear history. The Herschel-Bulkley viscosity model was utilized to provide a yield stress as observed by the measured data and previous rheology measurements. To approximate the partial wall slip, a semi-implicit, non-linear Navier slip law was implemented into the finite volume CFD package OpenFOAM (Weller et al., 1998) according to Ferrás et al. (Ferrás et al., 2013). The initial rheology measurements were performed with a standard plate-plate rotational rheometer with rather smooth plate surfaces (polished metal). However, these measurements turned out to be unsuitable for a fluid with pronounced wall slip. The influence of the rheological bulk characteristics and the apparent wall slip properties on the flow curve of the fluid cannot be accurately separated in such a rheological measurement setup as also demonstrated by Piau et al. (Piau, 2007). Thus, it was decided to recursively fit the modeling parameters of the bulk rheology model and the wall slip model to the measured reference data. As shown in Figure 3a, an increased zero-shear zone can be produced by providing a sufficient yield stress in the Herschel-Bulkley model. However, this also produces flat velocity profiles without velocity gradients in the central part of the velocity profiles, where the yield stress is not exceeded. In contrast, the measured velocity profiles show rather steep velocity gradients even close to the maximum velocity point, where the shear stress should be at its minimum.

Table 3: Parameters for the flow field imaging at the ZAB model

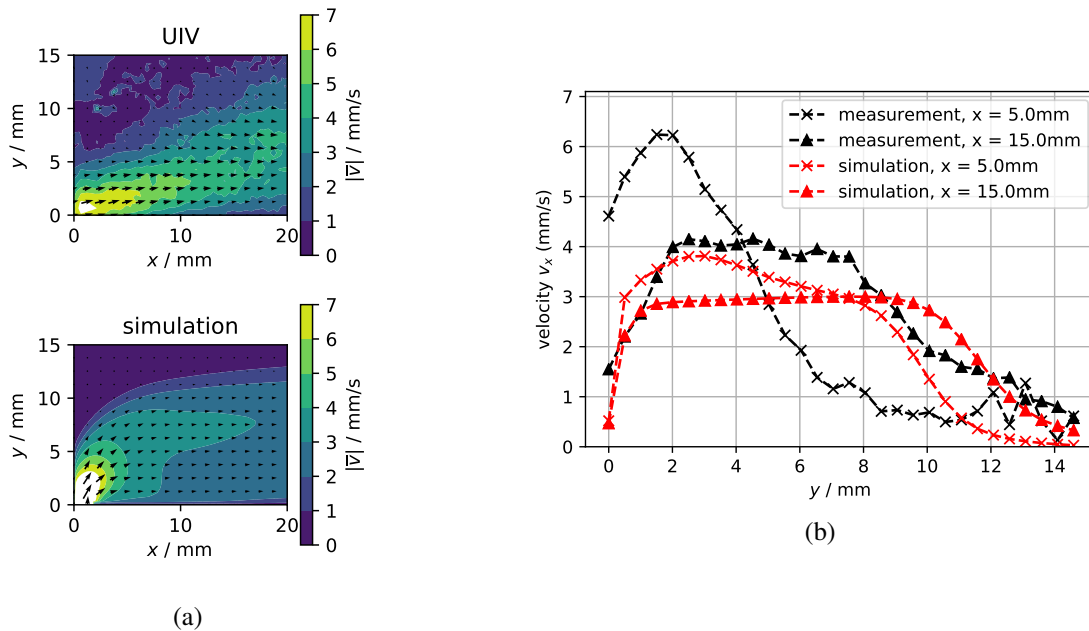|	
Number of us elements	50
Excitation frequency f	6 MHz
Signal length	2 periods
Pulse repetition frequency f_{prf}	600
Measurement time	50 s

(a)

(b)

Figure 3: (a) Measured (top) and simulated (bottom) flow field in the fluidic ZAB model. (b) Flow profiles of the x-component of the flow for selected x-positions.

5   Conclusion

We presented an experiment for the validation of numerical models for multiphase fluids with a moderately high particle concentration (in the order of 10 vol.-%). Ultrasound imaging velocimetry was successfully

applied to measure the two-dimensional and two-component flow field in a model of a zinc-air flow battery (ZAB) with a zinc suspension that is applicable for real working ZABs. A validation of the measurement system was conducted by comparing the ultrasound measurement to optical reference measurements and a CFD simulation with the optical transparent model fluid glycerin.

The measured flow field in the zinc suspension was compared to numerical simulations. The observed differences between the measurements and the simulation data leads to the assumption that this type of flow behavior cannot be accurately modeled with the utilized homogeneous, generalized Newtonian approach and that at least the shear history has a significant impact. Accordingly the numerical models will be extended to account for the shear history on one hand, and a more detailed multiphase approach (CFD-DEM) will be employed to further investigate the complex flow behavior. In the future, flow investigation at a real working ZAB are planned to correlate the measured flow field and the achieved power densities of the electrochemical cell.

References

Adrian RJ (2005) Twenty years of particle image velocimetry. *Experiments in Fluids* 39:159–169

Bohs LN, Geiman BJ, Anderson ME, Gebhart SC, and Trahey GE (2000) Speckle tracking for multi-dimensional flow estimation. *Ultrasonics* 38:369–375

Büttner L, Nauber R, Burger M, Räbiger D, Franke S, Eckert S, and Czarske J (2013) Dual-plane ultrasound flow measurements in liquid metals. *Measurement Science and Technology* 24:055302

Deen N, Annaland MVS, Van der Hoef MA, and Kuipers J (2007) Review of discrete particle modeling of fluidized beds. *Chemical engineering science* 62:28–44

Ferrás L, Nóbrega J, and Pinho F (2013) Implementation of slip boundary conditions in the finite volume method: new techniques. *International journal for numerical methods in fluids* 72:724–747

Mäder K, Nauber R, Galindo V, Beyer H, Büttner L, Eckert S, and Czarske J (2017) Phased array ultrasound system for planar flow mapping in liquid metals. *IEEE Transactions on Ultrasonics, Ferroelectrics, and Frequency Control*

Nauber R, Büttner L, Eckert K, Fröhlich J, Czarske J, and Heitkam S (2018) Ultrasonic measurements of the bulk flow field in foams. *Physical Review E* 97:013113

Piau J (2007) Carbopol gels: Elastoviscoplastic and slippery glasses made of individual swollen sponges: Meso-and macroscopic properties, constitutive equations and scaling laws. *Journal of non-newtonian fluid mechanics* 144:1–29

Poelma C (2017) Ultrasound imaging velocimetry: a review. *Experiments in Fluids* 58:3

Sapkota P and Kim H (2009) Zinc–air fuel cell, a potential candidate for alternative energy. *Journal of Industrial and Engineering Chemistry* 15:445–450

Smith KC, Chiang YM, and Carter WC (2014) Maximizing energetic efficiency in flow batteries utilizing non-newtonian fluids. *Journal of The Electrochemical Society* 161:A486–A496

Tanter M and Fink M (2014) Ultrafast imaging in biomedical ultrasound. *IEEE transactions on ultrasonics, ferroelectrics, and frequency control* 61:102–119

Taylor ZJ, Gurka R, Kopp GA, and Liberzon A (2010) Long-duration time-resolved piv to study unsteady aerodynamics. *IEEE Transactions on Instrumentation and Measurement* 59:3262–3269

Thieme N, Bönisch P, Meier D, Nauber R, Büttner L, Dadzis K, Pätzold O, Sylla L, and Czarske J (2017) Ultrasound flow mapping for the investigation of crystal growth. *IEEE transactions on ultrasonics, ferro-electrics, and frequency control* 64:725–735

Weller HG, Tabor G, Jasak H, and Fureby C (1998) A tensorial approach to computational continuum mechanics using object-oriented techniques. *Computers in physics* 12:620–631